Biointerface Research in Applied Chemistry
Platinum Open Access Journal (ISSN: 2069-5837)

Article
Volume 10, Issue 6, 2020, 7085 - 7096
https://doi.org/10.33263/BRIAC106.70857096

Optical, Structural, and Antimicrobial Study of Gold nanoparticles Synthesized Using an Aqueous Extract of *Mimusops elengi* Raw Fruits

Arpita Tripathy [1], Manoranjan Behera [2*], Ardhendu Sekhar Rout [1], Susanta Kumar Biswal [1], Ajit Dattatreya Phule [3]

[1] Department of Chemistry, Centurion University of Technology and Management, Odisha, India
[2] Department of Basic Sciences and Humanities, Silicon Institute of Technology, Bhubaneswar, Odisha, India
[3] Department of Chemical Engineering, Gyeongsang National University, Jinju, South Korea
* Correspondence: manoranjan@silicon.ac.in;

Scopus Author ID 7004588847
Received: 28.04.2020; Revised: 26.05.2020; Accepted: 28.05.2020; Published: 6.06.2020

Abstract: Gold nanoparticles (AuNPs) has been synthesized via a green route using an aqueous extract of *Mimusops elengi* raw fruits. The phytochemicals of the fruit help in stabilizing and capping of the nanoparticles. The formation and stability of the synthesized samples has been explained based on results that we obtain from UV-Visible spectroscopy, Fourier Transform Infra-Red (FTIR) spectroscopy, Dynamic Light Scattering (DLS), X-ray diffraction (XRD), scanning electron microscopy (SEM). Further, the positive results of the antimicrobial test add one more novelty to this work. The axiom of this work is the synthesis of stable AuNPs without using any external stabilizing or reducing agents. The formation of AuNPs with the help of photochemical present in *Mimusops elengi* is yet another important aspect of this work, which provides an eco-friendly method for the synthesis of AuNPs, which can be used extensively because of its non-hazardous condition.

Keywords: Nanoparticles; *Mimusops elengi* fruits; Gram-positive bacteria, Gram-negative bacteria.

1. Introduction

Biosynthesis of nanoparticles (NPs) is an emerging field that is receiving enormous attention from research communities these days. Biosynthesis of noble metal nanoparticles (NPs) like silver (Ag), gold (Au), platinum (Pt), palladium (Pd), etc. is a difficult task. In order to develop NPs of various morphologies and sizes, defining the production route and reaction conditions are of paramount importance. In recent years much effort has been put to develop metal NPs using micro-organisms and plant extract. The two essential strategies employed to synthesize NPs are: (1) *Top-down approach* and (2) *Bottom-up approach* [1-6]. In the synthesis of NPs, the various common conventional routes utilize environmentally toxic chemicals. So, nowadays research going on in the field of biology, chemistry, and materials science are adopting bio-directed synthesis (also known as green synthesis) of NPs. Green synthesis of NPs is an environmentally friendly method that avoids the use of toxic, carcinogenic, harsh, and expensive chemicals [1,4,7-9]. The various biological methods employ micro-organisms (algae, bacteria, fungi, yeast, etc.) and various plant parts in the synthesis of NPs [9-13]. Owing to cost-effectiveness and environmental friendliness, plant-mediated synthesis is widely used these days as an alternative route for large scale production of NPs. The various phytochemicals present in plant extracts do not only act as a reducing agent but also as a stabilizing agent in developing NPs [14-18].

There is a vast list of plants that were used in the synthesis of NPs. Some of them are *Centella asiatica, Averrhoa bilimbi Linn, Zingiber officinale, Pistacia integerrima, Mentha piperita Galaxaura elongate, Mimusops elengi,* etc. [9-13]. The various parts of plants that were used in the synthesis of NPs are leaves, stems, bark, flowers, fruits, roots, etc. Several metal NPs (i.e., Au, Ag, Pt, Pd, etc.) with potential applications in various fields such bio-medical, sensing, heat transfer, catalysis, etc. have been prepared by many researchers using plant extracts. Various parts of the plant have been used not only to obtain NPs from their precursor salts but also widely used as traditional Indian medicine for the treatment of many diseases [19]. We have chosen *Mimusops elengi* raw fruit extract in synthesizing gold nanoparticles (AuNPs). According to Ayurveda in India, the various parts of *Mimusops elengi* (known as *Bakul Tree*) are used as herbal medicine [16,19,20]. Das et al. [10] have synthesized Au NPs of well-defined size and distinct morphology using ethanolic leaf extract of *Centella asiatica*. Isaac et al. [21] have synthesized Au and Ag NPs using the fruit extract of *Averrhoa bilimbi Linn.* The surface Plasmon resonance band (SPR) found in the UV-visible spectra of liquid samples shows the formation of Au and Ag NPs. The presence of a single SPR band near 540 nm in the spectrum results from the formation of spherical Au NPs, whereas 2 to 3 SPR bands suggest the formation of anisotropic NPs (i.e., cubic, hexagonal, pentagonal, etc.). Further, with the help of FTIR spectra, they reported that the presence of phytochemicals in plant extract are responsible for the reduction of Au^{3+} and Ag^{+}-ions to respective NPs. Au NPs are synthesized using the aqueous extract of the watermelon grid and evaluated their antioxidant and antibacterial effects [12]. They reported that synthesized Au NPs exhibited potential antibacterial activity against five foodborne pathogens (i.e.., *B. cereus, Bacillus cereus; E. coli, Escherichia coli; L. monocytogenes, Listeria monocytogenes; S. aureus, Staphylococcus aureus; S. typhimurium, Salmonella typhimurium*.) The Au nano-colloids exhibited high synergistic activity against the standard antibiotics like kanamycin and rifampicin. Au NPs also possessed significant antioxidant and anti-proteasome inhibitory potential against standard antioxidants.

Kumar et al. [15] have synthesized Ag NPs using the finely grounded powder of *Mimusops elengi* fruit extract in water. They reported that the synthesized Ag NPs were act as antibacterial and antioxidant agents against *Staphylococcus aureus* (S. aureus) and *Escherichia coli* (E. coli). Also, the NPs are reported to act as good antioxidant against ascorbic acid. The bark extract of *Mimusops elengi* was used for the synthesis of Au NPs in the water at room temperature under very mild conditions [16]. They confirmed the formation of spherical NPs from the SPR band in the absorption spectra, which were lies between 536 and 541 nm regions and XRD pattern. They reported that polyphenols present in the bark extract acted as both reducing as well as the stabilizing agent. They varied the concentration of bark extract from 50 to 600 mg/L and took 10.42 mM gold salt ($HAuCl_4$) to develop Au NPs. This is the only literature available on the synthesis of Au NPs using only the bark extract of *Mimusops elengi Linn.* They have studied the catalytic activity of Au NPs. They have not reported the antimicrobial activity of Au NPs using *Mimusops elengi Linn.* bark extract.

So, after an intensive literature study, we planned to synthesize Au NPs using the *raw fruits extract* of *Mimusops elengi, L.* in water. To the best of our knowledge, this is the first work on the synthesis of Au NPs using $Au(OH)_3$ salt as a precursor salt and aqueous extract of *Mimusops elengi L.* raw fruits as the dispersion medium. We are also the first to report on antimicrobial activity of Au NPs in the presence of the aqueous extract of Mimusops *elengi L.* raw fruits.

2. Materials and Methods

2.1. Preparation of Mimusops elengi L. raw fruit extract in water.

Raw fruits were collected from the Bokul tree (*Mimusops elengi, L.*) present on the campus of *Silicon Institute of Technology, Bhubaneswar, Odisha*. Then, raw fruits weighing ~8.1 g was taken in a beaker containing 100 mL of deionized water (i.e., 81 mg/L) and placed in a hot magnetic stirrer plate maintained at 80 ^{0}C for 1.5 h. During the heating process, the beaker was covered with a watch glass to avoid loss of water. The aqueous extract was filtered using Whatman 42 (2.5 μm) and stored in a refrigerator maintained at ~10 ^{0}C. The extract is milky to the naked eye.

2.2. Preparation of gold salt solution in water.

Gold salt (gold (III) hydroxide) Au $(OH)_3$ of 79 % Au were purchased from Thermo Fisher Scientific to prepare Au NPs. The salt was dissolved in the calculated volume of nitric acid to form a solution of strength 32 μM.

2.3. Synthesis of gold NPs in the aqueous plant extract.

Freshly prepared aqueous fruit extract solution and the gold salt solution was used to synthesize Au nanofluids in water. At first, 5 mL of aqueous extract was taken in a beaker and placed in hot magnetic stirrer maintained at 70 ^{0}C. Then, the gold solution was added drop-wise using a micropipette into it under stirring condition. After 1 minute of hot stirring, we observed that the color of the solution has changed to violet-pink. It happens due to the formation of Au NPs in the extract. In this investigation, the Au-contents were varied as 19.80, 39.21, 58.25, 76.92, and 95.23 μM in the presence of a fixed volume (5 mL) of raw fruit extract in water.

2.4. Experimental measurements.

The optical absorption spectra of liquid samples in water were studied in the 200-900 nm regions by a UV-Visible spectrometer (Perkin-Elmer Lambda 750 spectrophotometer). To measure the data, samples were loaded in a quartz cell of 3 mm optical path length. The spectra were recorded against water taken as the reference. The machine automatically subtracts the reference spectrum from the sample and gives the resultant ones. The FTIR data studied in this work were measured in the 400 to 4000 cm^{-1} region of the vibrational frequencies for the various samples. Liquid solutions were studied in an attenuated total reflectance (ATR) mode using a ZnSe crystal as a sample holder with a Perkin-Elmer FTIR Spectrometer (Spectrum 65). The reported frequencies are accurate to ± 2 cm^{-1} in the case of the sharp bands and ± 5 cm^{-1} or even larger in the case of the broad bands. The zeta potential and hydrodynamic diameter of NPs were measured using a Malvern Nano Zetasizer Nano Z potential analyzer, which works on the micro-electrophoresis technology.

The crystalline structures of Au-NPs were analyzed in terms of the wide-angle XRD by using an X-ray diffractometer (PHILIPS model PW-1710). The nanocolloids were cast on the surface of the silicon substrate and placed in a sample holder in the diffractometer in order to measure the diffractogram from flat surfaces of the sample. The diffraction data were recorded using filtered monochromatic radiation of CuK_α of wavelength λ = 0.15405 nm through a Ni filter. The data were collected with a computer, which was interfaced through the

diffractometer, at a scanning speed of 0.05 ^{0}/s in applied voltage of 40 kV, and applied the current 20 mA. The range of the diffraction angle 2θ was varied from 10 to 100^0. Oxford model Leo1550 VP SEM was used to take the scanning electron microscopic (SEM) images. The images were taken at an accelerated voltage in the 2-10 kV range. The nanofluids were deposited on the surface of a silicon substrate and dried in desiccators. The samples were coated with a thin film of gold by a sputtering method to provide a conductive surface during the measurements. Then microscopic images were taken at selective scales of magnifications of some of the samples. Antimicrobial and antifungal activity of samples was studied using the agar well diffusion method. Using this test, one can know the antibiotic sensitivity of bacteria. We used agar well diffusion method to study antibacterial as well as antifungal effects of phyto-synthesized Au NPs. In order to study the antimicrobial effect, at first, wells were made using a sterile cork borer (5 mm) under aseptic condition. Then inocula were prepared by diluting the Au NPs solution (aqueous AuNPs) with 0.9% NaCl to a 0.5 McFarland standard. It was swabbed onto the plates, which were previously seeded by one of the tested pathogenic bacteria as well as fungi. Different concentrations of the Au NPs were loaded on marked wells with the help of micropipette under aseptic conditions, and plates were incubated at 37 ^{0}C, and incubation time was ~24 h. Then the diameter of zone of inhibition (ZOI) was measured using a ruler and expressed in mm.

3. Results and Discussion

3.1.UV-Vis and FTIR analysis.

We studied the UV-Vis optical absorption spectra in the 200–600 nm regions to verify the formation and stability of NPs in a biofluid. The UV-Vis spectra of five nanofluids consisting of (a) 19.80, (b) 39.21, (c) 58.25, (d) 76.92, and (e) 95.23 μM Au NPs in an aqueous raw fruit extract of *Mimusops elengi* were shown in Figure. 1A. During the synthesis, we observed color change due to the formation of Au NPs.The color change is ascribed to the Surface Plasmon Resonance phenomenon [14,22,23]. The free electrons present in metal NPs give the SPR absorption band due to the combined vibration of electrons of Au NPs in resonance with a light wave. We observed a broad SPR band near 540 nm for all our samples except for the extract. SPR band near 540 nm reveals the formation of Au NPs of size less than 100 nm [14].

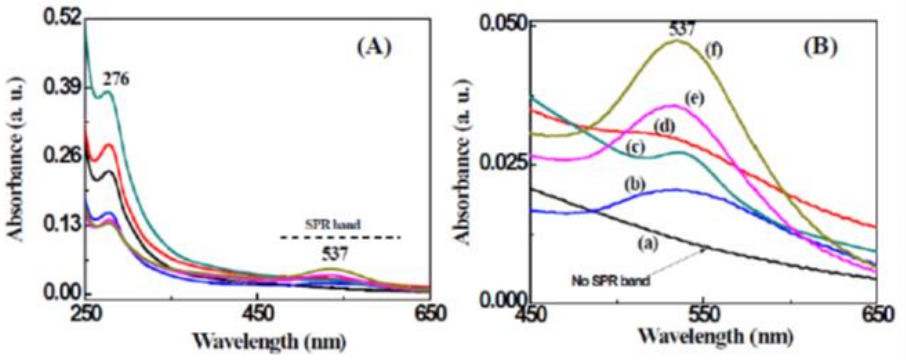

Figure 1. (A) The UV-Vis spectra of liquid samples consisting of (a) 19.80, (b) 39.21, (c) 58.25, (d) 76.92, and (e) 95.23 μM Au NPs in an aqueous fruit extract of *Mimusops elengi* and (B) shows only SPR band of samples (a-e).

From Figure 1, it is observed that with increasing the Au-content, the intensity of the SPR band also increases due to the presence of a large number of Au NPs in the biofluid. Also,

it is observed that the SPR band (see Figure. 1B.) is red-shifting with increasing in Au-content. It is due to an increase in the size of the Au cluster [7,14,22]. An increase in the Au cluster size causes dipole-dipole interaction and plasmonic coupling between aggregates [22]. The weak band observed near 276 nm is from n→π* electronic transition of the phytochemicals present in the plant extract [16].In an article, Majumdar et al. [16] have reported an SPR band near 540 nm for Au NPs. They have increased the *Mimusops elengi* bark extract concentration by keeping the Au content fixed. Here we studied the optical properties by varying the Au content and keeping the *Mimusops elengi* fruit extract concentration constant.

FTIR spectra were studied to know about the role of plant extract in the synthesis of Au NPs and also have an idea on any interfacial interaction that occurs between Au NPs and phytochemicals present in the extract. It also helps in identifying the capping capacity of phytochemicals present in the plant extract. The FTIR spectra of six liquid samples consisting of consisting of (a) 0, (b) 19.80, (c) 39.21, (d) 58.25, (e) 76.92, and (f) 95.23 μM Au NPs in an aqueous fruit extract of *Mimusops elengi*. were shown in Figure 2. The FTIR bands of plant extract without Au NPs was found at 3315 cm^{-1}, 2930 cm^{-1}, 1735 cm^{-1}, 1610 cm^{-1}, 1415 cm^{-1}, 1225 cm^{-1}, 1055 cm^{-1}, and 610 cm^{-1}. In the presence of Au NPs, it is found that the intensity of some band has increased, and some band either shifts towards longer wavelength/shorter wavelengths from their original position. An increase in band intensity and shifting of the band indicates the existence of interaction occurs between Au NPs and phytochemicals [3,7,14,23]. The band at 3340 cm^{-1}, 2928 cm^{-1}, 1618 $cm^{-1,}$ and 1050 cm^{-1} is due to O-H stretching, aldehydic C-H stretching, amide-I, -C-O-C- stretching vibration, respectively [23].

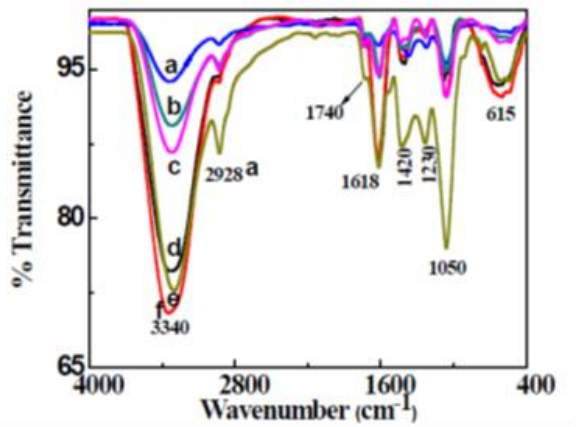

Figure 2. The FTIR spectra of liquid samples consisting of (a) 0, (b) 19.80, (c) 39.21, (d) 58.25, (e) 76.92, and (f) 95.23 μM Au NPs in an aqueous fruit extract of *Mimusops elengi*.

3.2. Structural analysis using XRD and SEM.

The crystalline nature of Au NPs was studied using the XRD pattern. The XRD patterns of the selected samples consisting of (a) 19.80, (b) 58.25, and (c) 95.23 μM Au NPs were shown in Figure 3A). For the XRD study, samples were dropped cast on a silicon substrate and dried at 70 ^{0} C. The characteristic diffraction peaks were observed at 37.5^0, 43.9^0, 63.9^0 and 77.7^0 in the 2θ range 30–80^0 which can be indexed to the (111), (200), (220) and (311) planes of face-centered cubic (*fcc*) Au-crystal, respectively [8,16,22,24]. The indexed planes have a good match with the standard diffraction pattern of JCPDS No. 04-0784. It reveals that the synthesized Au NPs are composed of pure crystalline gold. From the XRD-pattern, the intense peak corresponding to (200) plane than the other planes suggests that the (200) plane is in the main orientation.

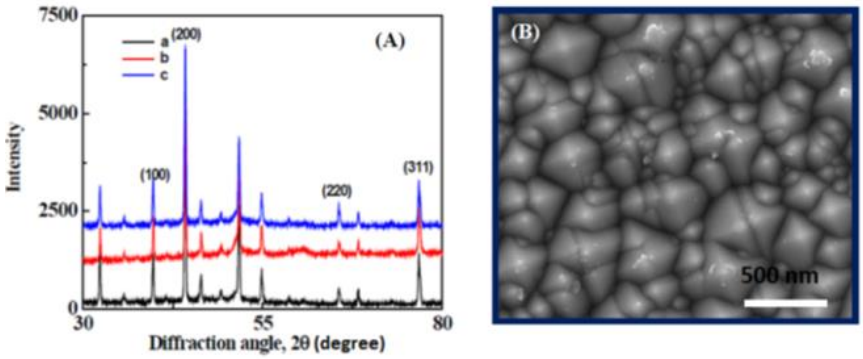

Figure 3. (A)XRD patterns of selective samples consisting of (a) 19.80, (b) 58.25, and (c) 95.23 μM Au NPs and (B) SEM image of a sample containing 95.23μM Au NPs.

SEM image gives information about the morphology, size details, and size distribution of the Au NPs. Figure 3B showed that the particles were of non-spherical in shape but the nano range. The size distribution is non-uniform that is polydispersity in nature. The large size may be due to the application of heat in order to remove the solvent during sample preparation or may be due to aging (as we took image after 1 month of sample preparation). Jafarizad et al. [17] have reported the formation of spherical Au NPs of size 100 nm. They have used different plant extracts than ours in the synthesis of Au NPs.

3.3. Hydrodynamic diameter and zeta potential analysis.

The particle size distribution of different samples consisting of (a) 19.80, (b) 39.21, (c) 58.25, (d) 76.92, and (e) 95.23 μM Au NPs in an aqueous fruit extract of *Mimusops elengi* were shown in Figure 4A. It is found from the spectra that the average hydrodynamic diameter for sample-a is100 nm. In contrast, it has increased to 156 nm in the sample-e. From the plot intensity Vs. size (Figure. 4B), it is found that the average size is increasing with increasing the Au content. This happens because as the Au content increases, the relative number of phytochemical molecules decreases. So, due to a relative decrease in the number of capping molecules, the capping efficiency decreases, and this causes an increase in the size of Au clusters [25-28]. Sujitha and Kannan [22] have reported an average hydrodynamic diameter of 50 nm for their samples using citrus fruit extract. Average size between 80-100 nm was reported by Vasanthraj et al. [29] for Au NPs synthesized using *R. tuberosa* extract.

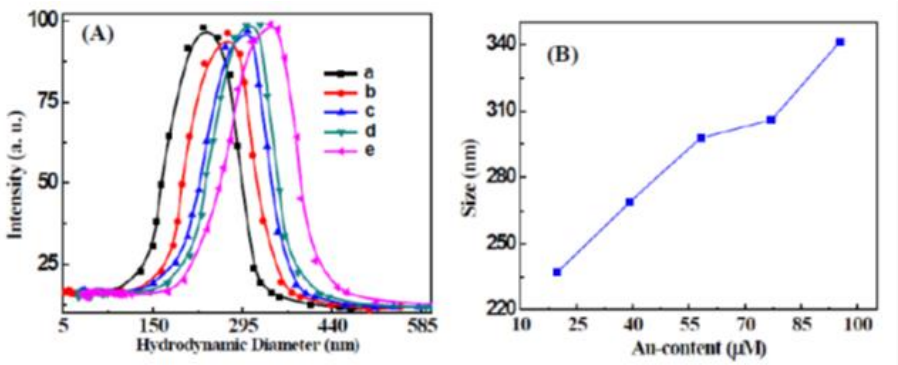

Figure 4. (A) Size distribution of liquid samples consisting of (a) 19.80, (b) 39.21, (c) 58.25, (d) 76.92, and (e) 95.23 μM Au NPs in an aqueous fruit extract of *Mimusops elengi* and (B) Variation of size (hydrodynamic diameter) with Au-content.

We also studied zeta potential distribution to have an idea about the colloidal stability of nano-colloids. Figure 5A Shows the zeta potential distribution of different samples

consisting of (a) 19.80, (b) 39.21, (c) 58.25, (d) 76.92, and (e) 95.23 μM Au NPs in an aqueous fruit extract of *Mimusops elengi*. zeta potential values are found to be negative for all the synthesized Au nanofluids. This shows that Au NPs are surrounded by the negative charge. We got the highest zeta potential of (-) 22.0 mV for a sample containing 19.80 μM Au NPs and lowest value for the sample containing 95.23 μM Au NPs. This implies that the size of NP is affecting the zeta potential. Size is smaller in sample-a, so its surface area is more and also its zeta potential value [25-28]. We also found from Fig. 5B that with an increase in Au-content or an increase in size, the zeta potential value decreases. Sujitha and Kannan [22] have reported average zeta potential of (-) 35.0 mV using citrus fruit extract. Vasanthraj et al. [29] have reported negative zeta potential (lies between -5 to -13 mV) for Au NPs using *R. tuberose* and *P. acidus* plant extract.

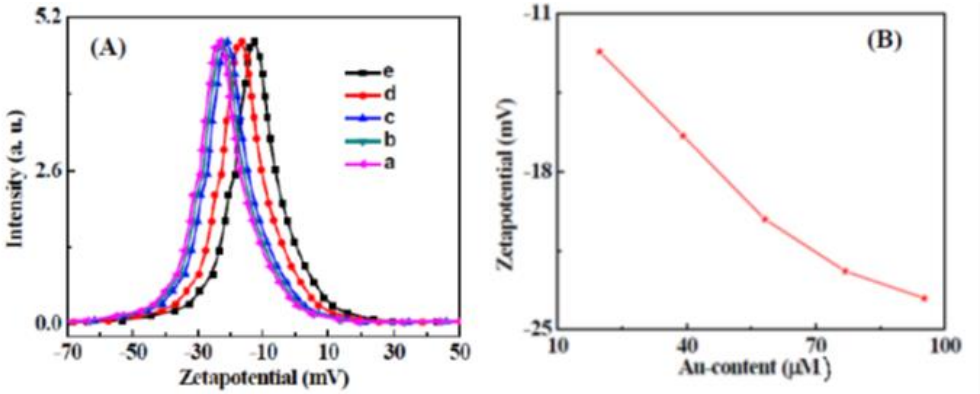

Figure 5. (A) Zetapotential distribution of liquid samples consisting of (a) 19.80, (b) 39.21, (c) 58.25, (d) 76.92, and (e) 95.23 μM Au NPs in an aqueous fruit extract of *Mimusops elengi* and (B) Variation of zetapotential with Au-content.

3.4. Analysis of the antibacterial activity of Au NPs with plant extract.

Two different pathogenic bacterial strains were used to study the antibacterial effect of prepared Au nanofluids. One strain was gram-positive bacteria (i.e., *Staphylococcus aureus*), and another was gram-negative bacteria (i.e., *Escherichia coli*). ZOI was found to be different for different samples.

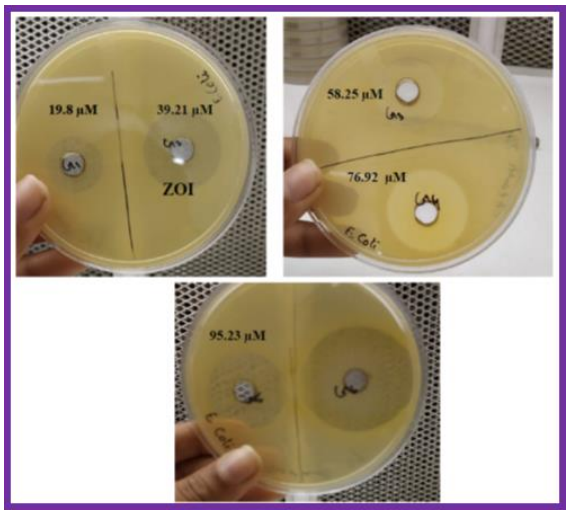

Figure 6. Antibacterial activity of Au NPs of various concentrations in aqueous medium against *E. Coli*.

There is no ZOI for negative control (i.e., for plant extract), and ZOI for the positive control (gold solution) is found to be 40 mm for both types of bacteria, which indicates that the

antibacterial property of the samples is because of the formation of Au NPs. Figure 6 shows the ZOI for samples consisting of (a) 19.80, (b) 39.21, (c) 58.25, (d) 76.92 and (c) 95.23 µM Au NPs against *Escherichia coli* was found to be 20 mm, 27 mm, 24 mm, 25 mm and 28 mm, respectively. So, maximum ZOI was found for the sample consisting of 95.23 µM Au NPs against gram-negative bacteria.

From the Figure 7, it is seen that the ZOI for samples consisting of (a) 19.80, (b) 39.21, (c) 58.25, (d) 76.92 and (c) 95.23 µM Au NPs against *Staphylococcus aureus* were found to be 21 mm, 31 mm, 27 mm, 33 mm and 26 mm, respectively. So, maximum ZOI was found for the sample consisting of 76.92 µM Au NPs against gram-positive bacteria. Abdel-Raouf et al. [14] have reported ZOI 17 mm, and 13 mm against gram-negative and gram-positive bacteria, respectively, for Au NPs synthesized using *Galaxaura elongate* in ethanolic extract. In another report, Bindu and Umadevi [30] mentioned that they had reported ZOI of ~13 mm for their Au NPs against gram-positive bacteria (i.e., *Staphylococcus aureus*). They have reported that the possible cause of death of bacteria in the presence of Au NPs either due to electrostatic interaction between Au NPs and cell surface of bacteria or due to penetration of active Au NPs into the bacteria.

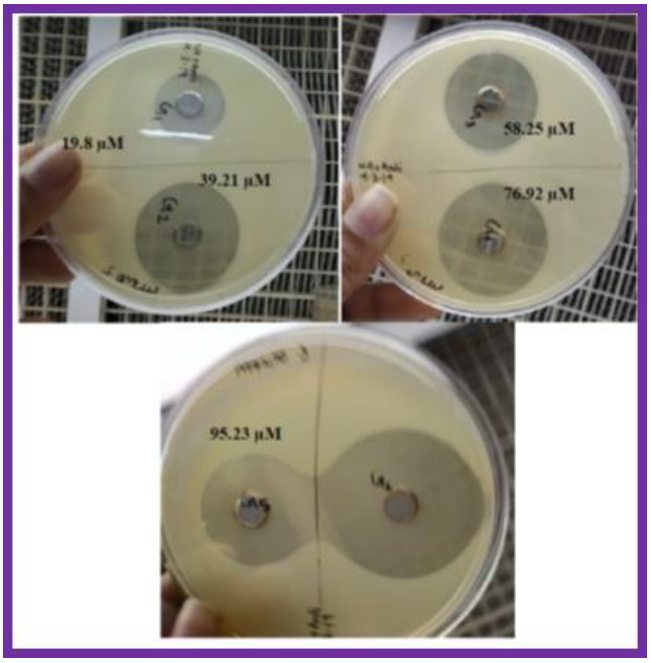

Figure 7. Antibacterial activity of Au NPs of various concentrations in an aqueous medium against *S. aureus*.

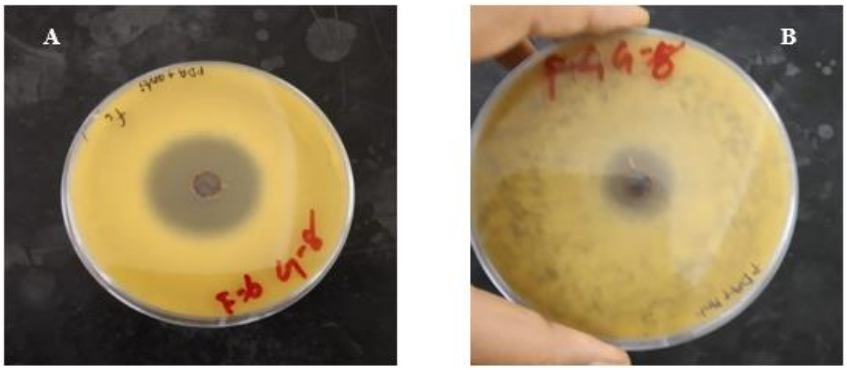

Figure 8. (A) Antifungal activity *Aspergillus tubingenesis*, **(B)** Antifungal activity against *Aspergillus niger*.

3.5. Analysis of the antifungal activity of Au NPs with plant extract.

For the study of antifungal properties, two fungi of class Eurotiomycetes: *Aspergillus niger* and *Aspergillus tubingenesis* were taken. The good diffusion method to study the antifungal effect of phyto-synthesized AuNPs was used. Here also, no ZOI for negative control (for plant extract) was found. At first, we took samples of concentration (a) 19.80, (b) 39.21, (c) 58.25, (d) 76.92 and (c) 95.23 µM AuNPs against both *Aspergillus niger* and *Aspergillus tubingenesis* and found that only 95.23 µM AuNPs shows ZOI against *Aspergillus tubingenesis* and not against *Aspergillus niger*, and it was found to be 15mm. Later by increasing the concentration of the samples, we get ZOI for both the fungi (Figure 8A & 8B).

3.6. Mechanism of formation of Au NPs.

It is reported that *Mimusops elengi L.* fruit is rich in quercitol, ursolic acid, dihydro quercetin, quercetin, β- d glycosides of beta-sitosterol, alpha spinasterol, mimusops acid and mimusopsic acid, mimugenone, pentacyclic triterpenes 3beta, 6beta, 19alpha,23-tetrahydroxy-urs-12-ene and 1beta-hydroxy-3beta-hexanoyllup-20 (29)-ene-23, 28-dioic acid, mimusops, mimus, mi-saponin A 16 alpha-hydroxy mi-saponin A, taxifolin, alpha-spinasterol glucoside, Miglycoside 1, mimusopside A and B and these polyphenolic compounds and can be utilized for the synthesis Au NPs from $HAuCl_4$ [31-33]. It is also reported that quercetin molecules present in the fruit plays an important role in the bioreduction of metal ions and 3.63±0.07 mg of quercetin equivalent/g of dry weight is present in the aqueous fruit extract of *Mimusops elengi* [6,34]. So, accordingly, we have proposed a scheme of formation of Au NPs in the presence of aqueous fruit extract. Quercetin (Scheme 1A) is a flavonoid with very strong chelating activity because it can chelate at three positions involving the carbonyl and hydroxyls at the C3 and C5 positions and the catechol group at the C3' and C4' site capable of reducing metal ion [6]. So the possible hypothetical mechanism is shown in Scheme 1B. The Au3+-ions accept electrons from the Quercetin molecules, thereby results in a reduction of these ins to form Au atoms. The Au-atoms later forms NPs by atoms-by atoms addition process, i.e., the bottom-up approach. The quercetin molecules not only help in reducing the process but also helps in stabilizing the Au NPs. Mathialagan and Mandal [35] have reported that quercetin molecules help in stabilizing metal NPs.

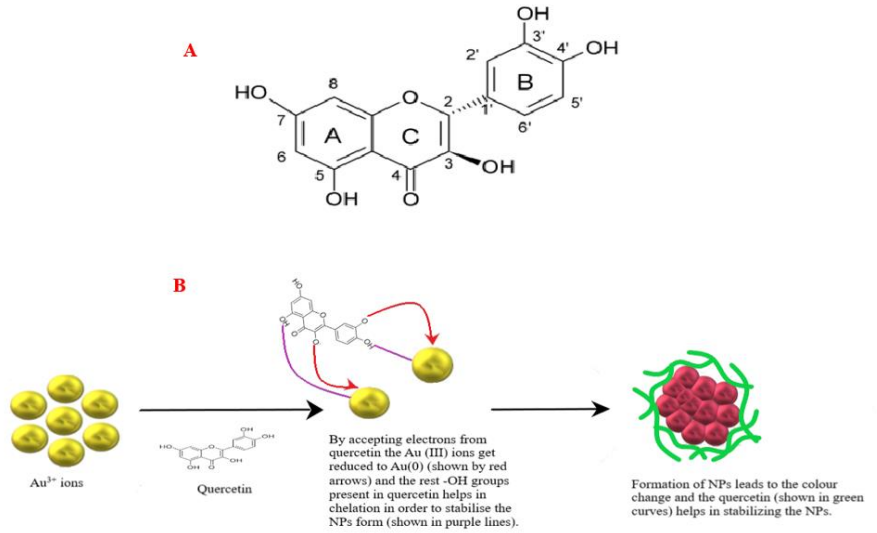

Scheme 1. (A) Structure of Quercetin molecule, **(B)** Proposed mechanism for the formation of Au NPs.

4. Conclusions

We have developed Au NPs using an aqueous raw fruit extract of *Mimusops elengi* tree for the first time. The synthesized Au NPs were characterized using UV-Vis, FTIR, XRD, DLS, SEM, and agar well diffusion method. UV-Vis spectral analysis and XRD analysis confirmed the formation of Au NPs using plant extract. The developed Au NPs sizes varied between 200-500 nm as confirmed from the DLS plot and SEM images. The Au NPs are polydisperse in nature and have a non-spherical shape. The antibacterial activity of the bio-synthesized Au NPs was evaluated against two (one gram-positive and one gram-negative) pathogenic bacteria and showed effective bactericidal activity. The maximum ZOI (33 mm) was found for the sample consisting of 76.92 μM Au NPs against gram-positive bacteria (*S. aureus*). We also proposed a plausible mechanism of the formation of Au NPs in support of the results.

Funding

This research received no external funding.

Acknowledgments

Support from Centurion University of Technology & Management, Odisha, India, and Silicon Institute of Technology, Bhubaneswar, India, is highly acknowledged.

Conflicts of Interest

The authors declare no conflict of interest.

References

1. Alex, S.; Tiwari, A. Functionalized gold nanoparticles: synthesis, properties and applications a review.*J Nanosci Nanotechnol* **2015**, *15***,**1869–1894, https://doi.org/10.1166/jnn.2015.9718.
2. Behera, M.; Ram, S. Intense quenching of fluorescence intensity of poly(vinyl pyrrolidone) molecules in presence of gold nanoparticles. *Appl Nanosci* **2013,** 3, 543−548, https://doi.org/10.1007/s13204-012-0159-8.
3. Behera, M.;Ram, S. Synthesis and characterization of core-shell gold nanoparticles with poly(vinyl pyrrolidone) from a new precursor salt. *Appl Nanosci* **2013**, 3, 83-87**,** https://doi.org/10.1007/s13204-012-0076-x.
4. Heiligtag, F.J.; Niederberger, M. The fascinating world of nanoparticle research. *Mater Today* **2013**, *16*, 262-271,https://doi.org/10.1016/j.mattod.2013.07.004**.**
5. Khan, I.; Saeed, K.; Khan, I. Nanoparticles: Properties, applications and toxicities. *Arabian J Chem* **2019**, *12*, 908-931,https://doi.org/10.1016/j.arabjc.2017.05.011**.**
6. Safenkova, I.V.; Zherdev, A.V.; Dzantiev, B.B. Using atomic force microscopy to assess surface modification of gold nanoparticles. *Biointerface Res App Chem* **2019**, *9*, 3894–3897, https://doi.org/10.33263/BRIAC92.894897.
7. Behera, M. Proposing a feasible mechanism to support the exhibition of superb colloidal stability of gold nanoparticles with poly (vinyl pyrrolidone) in the form of a nanofluid in N, N′-dimethyl formamide. *Res J Nanosci Nanotechno* **2015**, *5*, 60-73, http://doi.org/10.3923/rjnn.2015.60.73**.**
8. Behera, M. and Ram, S. Mechanism of solubilizing fullerene C_{60} in presence of poly(vinyl pyrrolidone) molecules in water. *Fuller Nanotub Car N* **2015**, *23*, 906-916, https://doi.org/10.1080/1536383X.2015.1041109.
9. Khosravi-Darani, K.; da Cruz, A. G.; Shamloo, E.; Abdimoghaddam, Z.; Mozafari, M. R. Green synthesis of metallic nanoparticles using algae and microalgae. *Lett Appl NanoBioSci* **2019**, *3*, 666-670, https://doi.org/10.33263/LIANBS83.666670.
10. Das, R.K.; Borthakur, B.B.; Bora, U. Green synthesis of gold nanoparticles using ethanolic leaf extract of Centella asiatica. *Materials Letters* **2010**, *64*, 1445-1447,https://doi.org/10.1007/s11706-011-0153-1**.**
11. Rimal Isaac, R.S.; Sakthive, G.; Murthy, C. Green synthesis of gold and silver nanoparticles using Averrhoa bilimbi fruit extract. *J Nanotech* **2013**, *2013*,https://doi.org/10.1155/2013/906592**.**

12. Patra, J.K.; Baek, K.H. Novel green synthesis of gold nanoparticles using Citrullus lanatus rind and investigation of proteasome inhibitory activity, antibacterial, and antioxidant potential. *Int. J Nanomedicine* **2015**, *10*, 72-53,https://doi.org/10.2147/IJN.S95483**.**
13. Kumar, K.P.; Paul, W.; Sharma, C.P. Green synthesis of gold nanoparticles with Zingiber officinale extract: characterization and blood compatibility *Process Biochem* **2011**, *46*, 2007-2013,https://doi.org/10.1016/j.procbio.2011.07.011.
14. Abdel-Raouf, N.; Al-Enazi, N.M.; Ibraheem, I.B. Green biosynthesis of gold nanoparticles using Galaxaura elongata and characterization of their antibacterial activity. *Arabian J Chem* **2017**, *10*, S3029-39, https://doi.org/10.1016/j.arabjc.2013.11.044.
15. Kiran Kumar, H.A.; Mandal, B.K.; Mohan Kumar, K.; Maddinedi, S.b.; Sai Kumar, T.; Madhiyazhagan, P.; Ghosh, A.R.Antimicrobial and antioxidant activities of Mimusops elengi seed extract mediated isotropic silver nanoparticles. *Spectrochim Acta A Mol Biomol Spectrosc* **2014**, *130*, 13-18,https://doi.org/10.1016/j.saa.2014.03.024.
16. Majumdar, R.; Bag, B.G.; Ghosh, P. *Mimusops elengi* bark extract mediated green synthesis of gold nanoparticles and study of its catalytic activity *Appl Nanosci* **2016**, *6*, 521-528,https://doi.org/10.1007/s13204-015-0454-2.
17. Jafarizad, A.; Safaee, K.; Gharibian, S.; Omidi, Y.; Ekinci, D. Biosynthesis and in-vitro study of gold nanoparticles using mentha and pelargonium extracts. *Procedia Mat Sci* **2015**, *11*, 224-230, https://doi.org/10.1016/j.mspro.2015.11.113.
18. Elia, P.; Zach, R.; Hazan, S.; Kolusheva, S.; Porat, Z.E.; Zeiri, Y. Green synthesis of gold nanoparticles using plant extracts as reducing agents. *Int J Nanomedicine* **2014**,*9*, 4007-4021,https://doi.org/10.2147/IJN.S57343.
19. Kumar, H.; Savaliya, M.; Biswas, S.; Nayak, P.G.; Maliyakkal, N.; Setty, M.M.; Gourishetti, K.; Pai, K.S. Assessment of the in vitro cytotoxicity and in vivo anti-tumor activity of the alcoholic stem bark extract/fractions of Mimusops elengi Linn. *Cytotechnology* **2016**,*68*, 861-877, https://doi.org/10.1007/s10616-014-9839-4.
20. Purnima, A.; Koti, B.C.; Thippeswamy, A.H.; Jaji, M.S.; Swamy, A.H.; Kurhe, Y.V. Antiinflammatory, analgesic and antipyretic activities of Mimusops elengi Linn. *Indian J Pharm Sci* **2010**, *72*, 480–485.
21. Isaac, R.S.; Sakthivel, G.; Murthy, C. Green synthesis of gold and silver nanoparticles using Averrhoa bilimbi fruit extract. *J Nanotech* **2013**; *2013*, https://doi.org/10.1155/2013/906592.
22. Sujitha, M.V.; Kannan, S. Green synthesis of gold nanoparticles using Citrus fruits (Citrus limon, Citrus reticulata and Citrus sinensis) aqueous extract and its characterization. *Spectrochim Acta A Mol Biomol Spectrosc* **2013**, *102*, 15-23,https://doi.org/10.1016/j.saa.2012.09.042**.**
23. Maleki, M.J.; Pourhassan-Moghaddam, M.; Karimi, A.; Akbarzadeh, A.; Zarghami, N.; Mohammadi,S. A. Synthesis, characterisation, and application of chamomile gold nanoparticles in molecular diagnostics: a new component for PCR kits. *Biointerface Res App Chem* **2019**, *9*, 4635-4641, https://doi.org/10.33263/BRIAC96.635641**.**
24. Mohamed, M.M.; Fouad, S.A.; Elshoky, H.A.; Mohammed, G.M.; Salaheldin, T.A. Antibacterial effect of gold nanoparticles against Corynebacterium pseudotuberculosis. *Int J Vet Sci Med* **2017**, *5*, 23-29, https://doi.org/10.1016/j.ijvsm.2017.02.003.
25. Behera, M.; Ram, S. Solubilization and stabilization of fullerene C_{60} in presence of poly(vinyl pyrrolidone) molecules in water. *J Incl Phenom Macrocycl Chem* **2012**, *72*, 233−239, https://doi.org/10.1007/s10847-011-9957-y.
26. Behera, M.; Ram, S. Inquiring the mechanism of formation, encapsulation, and stabilization of gold nanoparticles by Poly(vinyl pyrrolidone) molecules in 1-butanol. *Appl Nanosci* **2014,** *4*, 247−254, https://doi.org/10.1007/s13204-013-0198-9.
27. Behera, M. An intensive study on the optical, rheological and electrokinetic properties of polyvinyl alcohol-capped nanogold. *Int Nano Lett* **2015**, *5***,**161-169, https://doi.org/10.1007/s40089-015-0150-y.
28. Behera, M.; Ram, S. Poly(vinyl pyrrolidone) mediated solubilization and stabilization of fullerene C_{60} in the form of nanofluid in an alcoholic medium. *Fuller Nanotub Car N* **2015,** *23*, 1064-1072,https://doi.org/10.1080/1536383X.2015.1068295.
29. Vasantharaj, S.; Sripriya, N.; Shanmugavel, M.; Manikandan, E.; Gnanamani, A.; Senthilkumar, P. Surface active gold nanoparticles biosynthesis by new approach for bionanocatalytic activity. *J Photochem Photobiol B* **2018**, *179*,119-125,https://doi.org/10.1016/j.jphotobiol.2018.01.007.
30. Bindhu, M. R.; Umadevi, M. Antibacterial activities of green synthesized gold nanoparticles. *Mater Lett***2014**, *120*, 122-125, https://doi.org/10.1016/j.matlet.2014.01.108.
31. Rani, S.; Rahman, K. *Molsari* **(***Mimusops Elengi* Linn.): A Boon Drug Of Traditional Medicine.*IJPSR***2017**, *8*, 17-28, https://doi.org/10.13040/IJPSR.0975-8232.8(1).17-28.
32. Baliga, M.S.; Pai, R.J.; Bhat, H.P.; Palatty, P.L.; Boloor, R. Chemistry and medicinal properties of the Bakul (Mimusops elengi Linn):a review. Food Res Int **2011**, *44*, 1823–1829,http://dx.doi.org/10.1016/j.foodres.2011.01.063.

33. Gami, B.; Pathak, S.; Parabia, M. Ethnobotanical, phytochemical and pharmacological review of Mimusops elengi Linn. *Asian Pac J Trop Biomed* **2012**, *2*,743-748, https://doi.org/10.1016/S2221-1691(12)60221-4.
34. Mathur, R.;Vijayvergia, R. Determination Of Total Flavonoid And Phenol Content In Mimusops Elengi Linn., IJPSR **2019**, *8*, 5282-85, https://doi.org/10.13040/IJPSR.0975-8232.8(12).5282-85.
35. Mathiyalagan, Siva; Mandal, B. K. Preparation of metal doped quercetin nanoparticles, characterization and their stability study. *Lett Appl NanoBioSci* **2019**, *8*,704–710, https://doi.org/10.33263/LIANBS84.704710.